Geochemical and geochronological characterization of Grand Mesa Volcanic Field, western Colorado

R. Cole, A. Stork, W. Hood, and M. Heizler
2017, pp. 103-113. https://doi.org/10.56577/FFC-68.103
Supplemental data: https://nmgs.nmt.edu/repository/index.cfml?rid=2017004

in:
The Geology of the Ouray-Silverton Area, Karlstrom, Karl E.; Gonzales, David A.; Zimmerer, Matthew J.; Heizler, Matthew; Ulmer-Scholle, Dana S., New Mexico Geological Society 68 th Annual Fall Field Conference Guidebook, 219 p. https://doi.org/10.56577/FFC-68

This page is intentionally left blank to maintain order of facing pages.

New Mexico Geological Society Guidebook, 68th Field Conference, Geology of the Ouray-Silverton Area, 2017, p. 103-113.

GEOCHEMICAL AND GEOCHRONOLOGICAL CHARACTERIZATION OF GRAND MESA VOLCANIC FIELD, WESTERN COLORADO

Rex Cole[1], Allen Stork[2], William Hood[1], and Matt Heizler[3]

[1]Department of Physical and Environmental Sciences, Colorado Mesa University, 1100 North Ave., Grand Junction, CO 81501, rcole@coloradomesa.edu;
[2]Department of Natural and Environmental Sciences, Western State Colorado University, 600 North Adams Street, Gunnison, CO 81231;
[3]New Mexico Bureau of Geology, New Mexico Institute of Mining and Technology, 801 Leroy Place, Socorro, NM, 87801

Abstract—The Grand Mesa Volcanic Field (GMVF) in western Colorado covers about 166 km^2 and ranges in elevation from 3452 (east) to 3000 m (west). Miocene (?) and Eocene strata underlie the basaltic lavas. The field can be subdivided topographically and geochemically into three areas: Western Tableland (WT), Crag Crest-Crag Crest Bulge (CC-CCB), and Ridge and Peak (RAP). Data for this study are based on 29 whole-rock $^{40}Ar/^{39}Ar$ dates, 81 ICP-MS analyses, and 404 ED-XRF analyses of samples collected at 46 locations. Dates range from 10.92±0.24 to 9.63±0.16 Ma, with a possible bimodal distribution. Age values for the dike and flow samples in the RAP area (N=9) range from 10.49±0.06 to 9.99±0.01 Ma, whereas the dike and flow samples in the CC-CCB area (N=4) are between 10.74±0.05 to 10.52±0.05 Ma. The flow samples from the WT area (N=16) range from 10.92±0.24 to 9.63±0.16 Ma. Major-element-oxide values from both ICP-MS and ED-XRF analyses show geographic partitioning. Samples from the CC-CCB area are noticeably enriched in silica, potassium, and phosphorous compared to those from the WT and RAP areas. Using a TAS classification, the CC-CCB samples are mostly shoshonite with minor latite, whereas the WT and RAP samples are mostly basaltic andesite and basalt. Chemo-stratigraphic variations documented in a drill core in the WT area, suggest that both magmatic differentiation and injection of new magma occurred during eruption of the flow sequence. The CC-CCB area has the only well-defined vent complex, consisting of a large discontinuously exposed dike and associated pyroclastics. The chronological and geochemical correlation of this complex to flows in the WT and RAP is not well understood. Additional undiscovered vent areas are likely present.

INTRODUCTION

Objective

The objective of this paper is to summarize the geochronological and geochemical characteristics the basaltic lava flows and dikes that make up the GMVF, and to describe a new vent area. Because this is a summary paper, only selected parts of the database are presented.

Field Area

Grand Mesa is a large erosional landform that dominates the skyline of western Colorado (Fig. 1). The greater Grand Mesa area stretches 67 km from Palisade, CO, on the west, to Electric Mountain on the east, and is bounded by the Colorado and Gunnison Rivers and their tributaries. The GMVF occupies the highest parts (3452 to 3000 m) of the greater Grand Mesa area and is about 54 km long and 22 km wide. The GMVF lavas have protected the underlying sedimentary rocks from erosion, creating a classic example of topographic inversion (Young and Young, 1968; Yeend, 1969, Aslan et al., 2008, 2010).

In this paper, the GMVF is subdivided into four areas (Fig. 2): (1) Western Tableland; (2) Crag Crest-Crag Crest Bulge; (3) Ridge and Peak; and (4) Landslide Bench. The Western Tableland (WT) gives Grand Mesa its characteristic profile and has an area of approximately 135 km^2. It represents the main lava-flow mass, which rests unconformably (?) on the Miocene (?) Goodenough formation (informal designation by Cole et al., 2013), the Eocene Green River Formation, and Uinta Formation (rare). The WT area has a "Y" shape defined by Palisade lobe (PL) and Flowing Park lobe (FPL), which merge into the "Stem" of the "Y." The Crag Crest-Crag Crest Bulge (CC-CCB) area is higher than the WT, ranging from 3305 to 3410 m (Fig. 2). Crag Crest Bulge (CCB), which is about 1.8 km long, is connected to Crag Crest Ridge (CCR), which is 4.0 km long and exposes up to 186 m of contorted, poorly defined lava flows. Significant talus occurs along the base of CCB and CCR.

The Ridge and Peak (RAP) area consists of lava-flow remnants that extend from the easternmost tip of CCR (called Finch Ridge) to Electric Mountain, including Leon Peak (LP), Green Mountain (GM), Priest Mountain (PM), Mt. Hatten (MH), Crater Peak (CP), and Mt. Darline (MD) (Figs. 1 and 2). The combined surface area of these highlands is conservatively estimated to be about 25 km^2. Crater Peak is the highest point (3452 m). Dikes large enough to show on regional geologic maps (Tweto et al., 1976a, 1976b; Tweto, 1979) occur at Lombard Ridge (LR), Chimney Rocks Ridge (CRR), and Little Dyke Creek (LDC), and a basaltic plug crops out at Iron Point (IP) (Fig. 1). Only the LR and CRR dikes are included in this study. Pleistocene glaciation has strongly influenced the RAP area (Yeend, 1969).

Numerous slump blocks form landslide benches around the WT, CC-CCB, and RAP areas (Fig. 2). The mass wasting that created these benches began during the late Pliocene and accel-

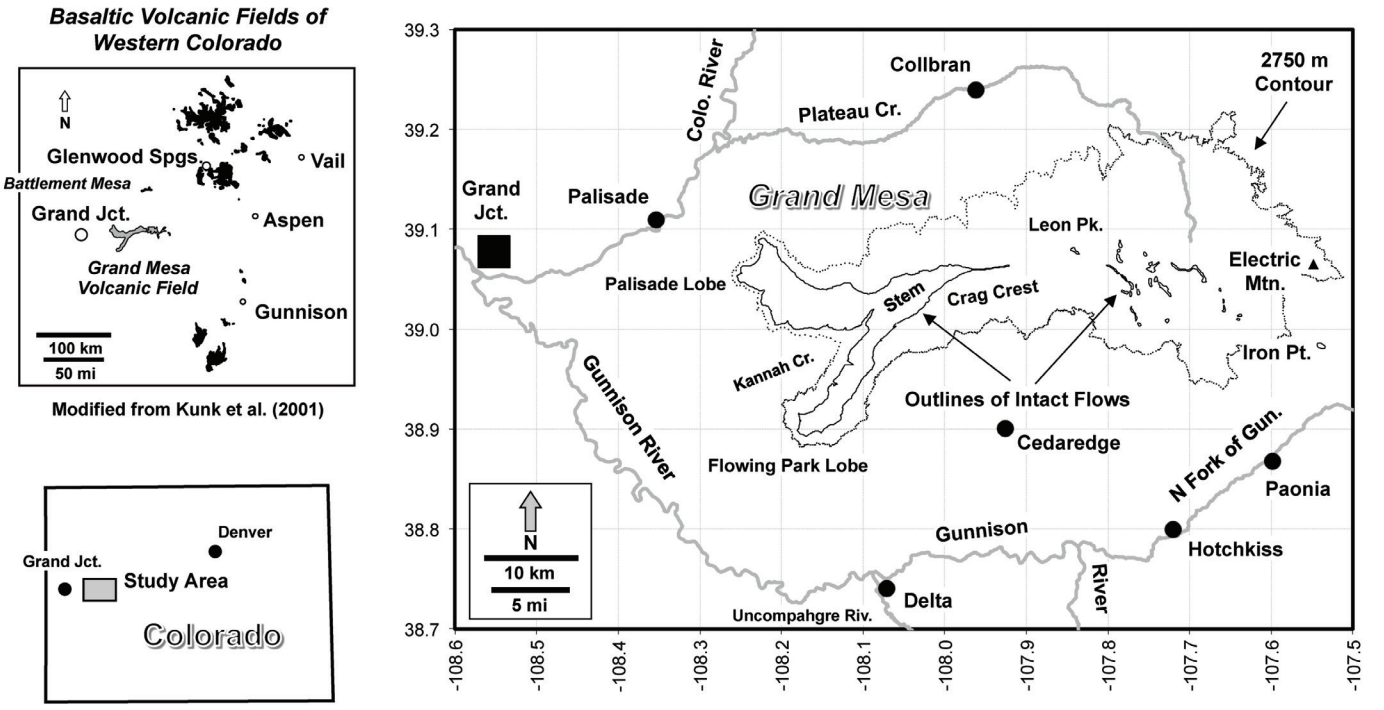

FIGURE 1. Index maps for the project area. The large map shows the outline of remnant basaltic flows of the GMVF and associated cultural features. Insert map in upper left shows the general location of GMVF in respect to other fields in northwestern and north-central Colorado (modified from Kunk et al., 2002). Note that the GMVF occupies only the higher elevations of the greater Grand Mesa area.

erated during Pleistocene ice loading (Young and Young, 1968; Yeend, 1969, 1973; Baum and Odum, 1996, 2003; Baum et al., 2007). The slumping has greatly complicated reconstruction of the GMVF and definition of its volcanic history (Green and Cole, 2016).

Volcanic History and Background

Volcanism that created the GMVF is associated with large-scale, mantle-driven, dynamic processes related to uplift of the Colorado Plateau and Southern Rocky Mountains, and creation of the Rio Grande Rift (Karlstrom et al., 2005, 2012 and references therein). Basaltic volcanism in north-central and northwest Colorado began approximately 26 Ma and continued intermittently into the Holocene (Larson et al., 1975; Leat et al., 1988, 1989; Budahn et al., 2002; Kunk et al, 2002; Day and Bove, 2004). Five eruption stages are defined by radiometric dating: (1) 24-22 Ma, (2) 16-13 Ma, (3) 11-9 Ma, (4) 8-7 Ma, and (5) <4 Ma (Kunk et al., 2002). Stage 3 volcanism produced the GMVF, nearby Battlement Mesa Volcanic Field, and most of the Glenwood Springs Volcanic Field (Fig. 1). The GMVF may have covered about 1300 km^2 at one time (Budahn et al., 2002), but in-situ remnants (i.e., WT, CC-CCB, and RAP areas) have a present-day footprint of only about 166 km^2.

The geochemical complexity of late Cenozoic basaltic rocks in northwest Colorado was first recognized by Larson et al. (1975) and Leat et al. (1988). Unruh et al. (2001), Budahn et al. (2002), and Stork (2006) further documented these geochemical and petrological variations in many of the fields in north-central and northwest Colorado (Fig. 1), but did not present data for GMVF. Beginning in about 2008, co-authors Stork and Cole began sampling outcrops, roadcuts, and drill core at many areas across the GMVF and found similar geochemical variations, as summarized in Cole et al. (2010, 2016).

GEOCHRONOLOGY

For many years, the age of the GMVF was placed at 9.7±0.5 Ma, based on a single $^{40}K/^{40}Ar$ date (Marvin et al., 1966). Although this date is considered accurate, it does not reflect the much broader range of values recognized today. Currently, age control for the GMVF consists of 31 $^{40}Ar/^{39}Ar$ dates (Table 1). Eleven whole-rock samples were dated at the geochronology laboratory of the U.S. Geological Survey (Kunk and Snee, 1998; Kunk et al., 2001, 2002) and 20 at the New Mexico Geochronology Research Laboratory (NMGRL). The 11 U.S. Geological Survey ages are from lava flows at Skyway (N=8) and Lands End (N=3), which are both in the WT area (Fig. 3). At the Skyway roadcuts, which is along Colorado Highway 65 near the Mesa Lakes, a section measured during the present study shows that at least 23 flows are exposed with a total thickness of about 93 m. The U.S. Geological Survey samples at Skyway appear to bracket the total flow thickness, although some flows were not sampled. The three Lands End samples were collected along roadcuts of U.S. Forest Service Road 100. A measured section at Lands End for the present study identified six flows with a total thickness of 64 m. The elevations provided in Kunk et al. (2001) suggest that the bottom, top, and middle parts of the sequence were sampled at Lands End; however, the coordinates given for the samples appear to be in

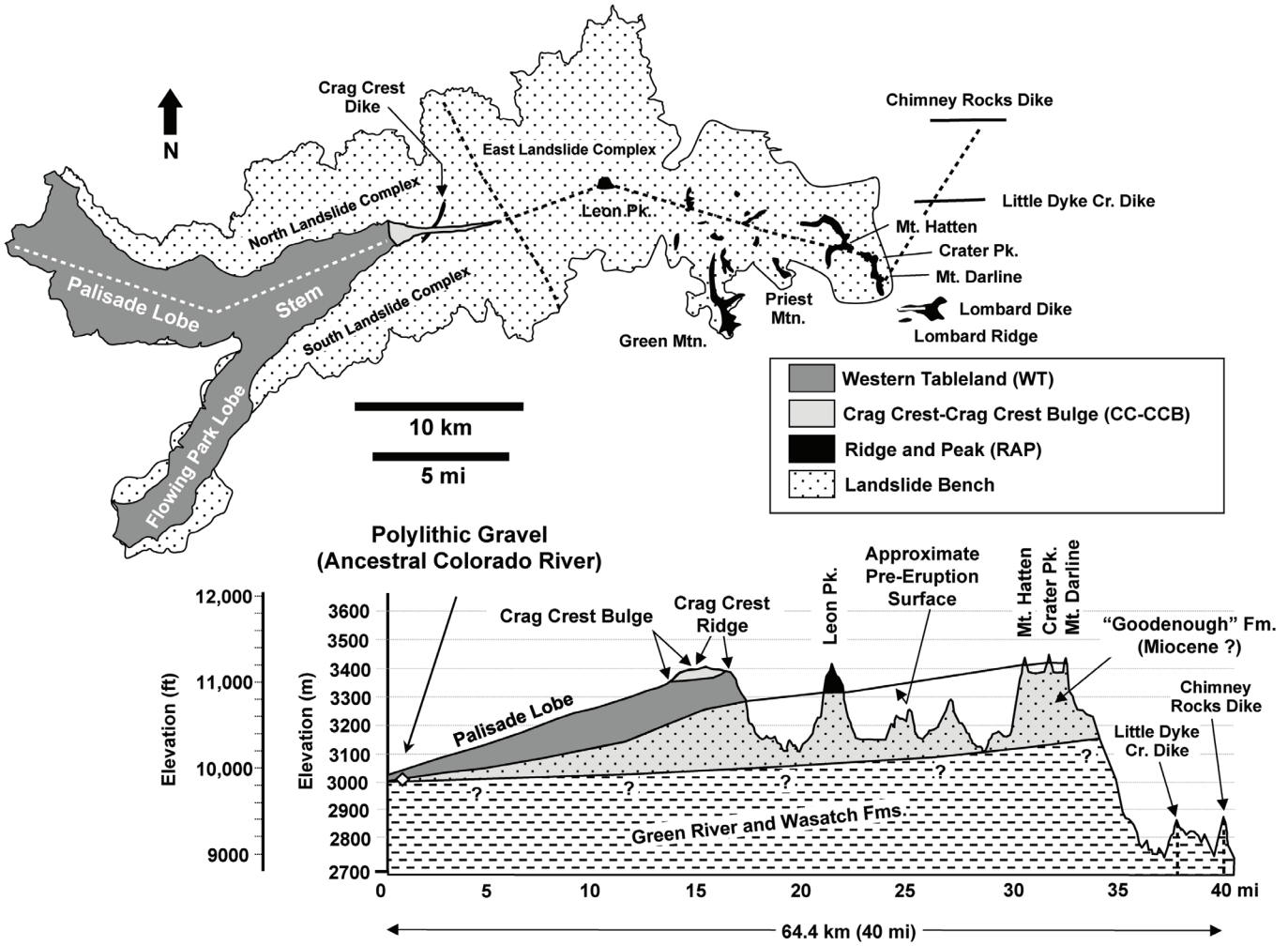

FIGURE 2. Physiographic components of the greater Grand Mesa area and diagrammatic east-west topographic-stratigraphic cross section. The WT area consists of the PL, FPL, and the "Stem." The RAP area consists of scattered flow remnants, such as LP, MH, CP, and MD. The 2750-meter line is the approximate outer limit of the landslide benches that surround the intact flows. The "Goodenough" formation, which underlies most of the GMVF, is an informal unit. It is up to 300 m thick, and consists of variegated bentonitic mudrock, chert-bearing limestone (rare), lithic granule-cobble conglomerate, and fine- to very coarse-grained lithic sandstone and conglomeratic sandstone (Cole et al., 2013).

error. Regarding the Kunk et al. (2001, 2002) dates, it should be noted that one sample at Skyway (K98-9-18A3&A4) and one sample at Lands End (K98-8-18G2&G5) have anomalously young ages (9.36 and 9.57 Ma, respectively; Table 1) when compared to with superjacent and subjacent samples at these locations. Both dates were from total-gas analysis (Kunk, et al., 2001), and no uncertainty values were given. Thus, we have discarded both samples from the discussions that follow, but include them on Figures 4 and 5 and in Table 1 for completeness.

In the present study, samples for whole-rock $^{40}Ar/^{39}Ar$ dating (N=20) were collected from across the GMVF (Fig. 3). The methodology and details for the data are provided in the Supplementary Documentation. In the WT area, seven samples came from FPL (N=2), Palisade Point (N=1), the D-9 core (N=3), and at "East Stem" (N=1) above Grand Mesa Lodge. The D-9 core (archived at CMU) was part of a nine-hole ground-water investigation by the U.S. Bureau of Reclamation (K. Weston, unpubl. report by U.S. Bureau of Reclamation, 1987). Four samples were collected from CC-CCB; two are from flows (top and bottom of the exposed sequence) and two are from a major dike. Nine samples from the RAP area were collected at Finch Ridge (N=1), LP (N=2), MH (N=1), CP (N=1), MD (N=2), LR (N=1), and CRR (N=1). All of the RAP samples are from flows except those at LR and CRR, which are from large dikes.

Results

Figure 4 summarizes the $^{40}Ar/^{39}Ar$ data for GMVF. Disregarding samples K98-9-18A3&A4 and K98-8-18G2&G5 from Skyway and Lands End, respectively, the restricted data set (N=29) values range from 10.92±0.24 to 9.63±0.16 Ma (1.29 Ma), with a mean of 10.28 Ma, a median of 10.23 Ma, and a standard deviation of 0.30 Ma. The distribution of dates (Fig. 4) has two principle modes at 10.53±0.01 Ma (N=7; MSWD=1.04) and 10.14±0.02 Ma (N=10; MSWD=0.75).

The geographic distribution of $^{40}Ar/^{39}Ar$ dates across the GMVF (Figs. 4 and 5) shows some subtle differences. Dates

TABLE 1. Summary of $^{40}Ar/^{39}Ar$ dates for the GMVF. Data from Skyway (Mesa Lakes) and Lands End are from Kunk et al. (2001, 2002). For comparison, all values have been normalized to a Fish Canyon Tuff sanidine age of 28.201 Ma. Two samples (K-98-8-A3&A4 at Skyway and K-98-81G2&G5 at Lands End) from Kunk et al. (2002) are listed in this table and posted on Figures 4 and 5, but are not used in the narrative of this paper. Dates for these two samples are based on total-gas analysis and no uncertainty is given. Note that the coordinates for the three Lands End samples are in error; the values given in Kunk et al. (2001) plot about 600 m west of the roadcuts. The remaining dates were generated at the New Mexico Geochronology Research Laboratory. Abbreviations: WT, Western Tableland; CC-CCB, Crag Crest-Crag Crest Bulge; RAP, Ridge and Peak.

Sample	Location	Remarks	Age (Ma)*	Latitude	Longitude	Elev.
Samples Analyzed by the U.S. Geological Survey (Kunk et al., 2001, 2002):						
K-98-8-18F2&3 (WT)	Skyway Roadcut	Flow	9.63±0.16	39º 2.51'N	108º 4.00'W	3243 m
K-98-8-19E4&5 (WT)	Skyway Roadcut	Flow	9.85±0.03	39º 2.80'N	108º 3.97'W	3219 m
K-98-8-18D1 (WT)	Skyway Roadcut	Flow	10.10±0.28	39º 2.93'N	108º 3.94'W	3206 m
K-98-8-18C1&2 (WT)	Skyway Roadcut	Flow	10.11±0.15	39º 3.02'N	108º 3.92'W	3200 m
K-98-8-18B1&2 (WT)	Skyway Roadcut	Flow	10.11±0.04	39º 3.05'N	108º 3.88'W	3197 m
K-98-8-18A3&4 (WT)	Skyway Roadcut	Flow	9.36 ?	39º 3.08'N	108º 3.83'W	3194 m
K-98-8-18B6 (WT)	Skyway Roadcut	Flow	10.12±0.04	39º 3.15'N	108º 3.67'W	3182 m
K-98-8-17A4 (WT)	Skyway Roadcut	Flow	10.47±0.13	39º 3.17'N	108º 3.58'W	3170 m
K-98-8-18I1&I4 (WT)	Lands End Roadcut	Flow	10.50±0.04	39º 1.48'N ?	108º 13.78'W ?	3011 m ?
K-98-8-18H4 (WT)	Lands End Roadcut	Flow	10.92±0.24	39º 1.46'N ?	108º 13.72'W ?	2999 m ?
K-98-8-18G2&G5 (WT)	Lands End Roadcut	Flow	9.57 ?	39º 1.43'N ?	108º 13.57'W ?	2987 m ?
Samples Analyzed by the New Mexico Geochronology Research Laboratory:						
GM-1 (WT)	Palisade Point	Lowest flow	10.57±0.01	39º 2.78'N	108º 15.08'W	2946 m
RC07-GM-B7 (WT)	Flowing Park	Lowest flow	10.05 ±0.06	38º 54.82'N	108º 7.67'W	3059 m
RC07-GM-B6 (WT)	Flowing Park	Highest flow	9.82 ±0.05	38º 56.13'N	108º 6.70'W	3076 m
DH-9 (WT)	D-9 Core	Flow at 43.3 m	10.14±0.04	39º 1.69'N	108º 3.80'W	3194 m
DH-9 (WT)	D-9 Core	Flow at 142.0 m	10.56±0.08	39º 1.69'N	108º 3.80'W	3095 m
DH-9 (WT)	D-9 Core	Flow at 143.3 m	10.32±0.09	39º 1.69'N	108º 3.80'W	3094 m
GC-139 (WT)	East Stem	Upper flow	9.86±0.02	39º 3.10'N	107º 59.30'W	3288 m
CC-1 (CC-CCB)	Crag Crest Ridge	Dike	10.52±0.05	39º 3.66'N	107º 57.81'W	3292 m
CC-2 (CC-CCB)	Crag Crest Ridge	Lowest flow	10.74±0.05	39º 3.65'N	107º 57.78'W	3298 m
GCX-74 (CC-CCB)	Crag Crest Ridge	Highest flow	10.54 ±0.01	39º 3.61'N	107º 57.58'W	3368 m
CC-3 (CC-CCB)	Quarry Knob	Dike	10.67±0.06	39º 4.45'N	107º 57.42'W	3176 m
GC-34 (RAP)	Finch Ridge	Flow	9.99±0.01	39º 3.76'N	107º 55.63'W	3358 m
RC07-GM-B5 (RAP)	Leon Peak	Lowest flow	10.45±0.04	39º 4.71'N	107º 50.39'W	3347 m
RC07-GM-B4 (RAP)	Leon Peak	Highest flow	10.16±0.04	39º 4.78'N	107º 50.63'W	3391 m
RC07-GM-B2 (RAP)	Mt. Darline	Lowest flow	10.39±0.05	39º 1.76'N	107º 39.45'W	3430 m
RC07-GM-B3 (RAP)	Mt. Darline	Highest flow	10.22±0.11	39º 1.77'N	107º 39.47'W	3446 m
RC07-GM-B10	Mt. Hatten	Highest flow	10.32±0.06	39º 2.94'N	107º 40.87'W	3422 m
RC07-GM-B11	Crater Peak	Lowest flow	10.49±0.06	39º 2.39'N	107º 39.80'W	3418 m
LBR-1	Lombard Ridge	Dike	10.23±0.04	39º 0.82'N	107º 38.45'W	3246 m
RC07-GM-D1	Chimney Rocks	Dike	10.18±0.05	39º 7.18'N	107º 35.66'W	2828 m

*All ages adjusted to Fish Canyon Tuff sanidine standard at 28.201 Ma. The uncertainty values are one sigma.

in the WT area range from 10.92±0.24 Ma to 9.63±0.16 Ma, with a mean of 10.20 Ma, a median of 10.11 Ma, and a standard deviation of 0.34 Ma. Dates from the CC-CCB show the tightest grouping for all of GMVF, with a range of 10.74±0.05 Ma to 10.52±0.05 Ma, a mean of 10.62 Ma, a median of 10.61 Ma, and a standard deviation of 0.11 Ma. The dates from the RAP area also have a relatively narrow spread, with a range of 10.49±0.06 Ma to 9.99±0.01 Ma, a mean of 10.27 Ma, a median of 10.23 Ma, and a standard deviation of 0.16 Ma (Fig. 4).

Discussion

It should be noted that the date at Palisade Point (10.57±0.01 Ma; Table 1) is a significant control point for understanding the timing of the topographic reversal that created the Grand Mesa landform, and the erosional history of the ancestral upper Colorado River (Aslan et al., 2008, 2010; Cole, 2011). The lava flow at Palisade Point rests on polylithic, unconsolidated river gravel (Fig. 2) that is compositionally similar to the modern Colorado River in the Grand Junction area. At a scattering of locations in the WT and RAP areas, lava flows rest on unconsolidated gravels of the Goodenough formation, which are dominated by diorite and andesite clasts (Cole et al., 2013) that probably came from the West Elk and Elk Mountains. It is also worth noting that Roebeck (2005) established $^{40}Ar/^{39}Ar$ dates (analysis by NMGRL) for the LDC dike (6.75±0.15 Ma) and IP plug (14.7±1.1 Ma) on the eastern margin of the GMVF (Fig. 1). Thus, they do not correspond to the any of the dates from this study (Table 1). Roebeck (2005) also provides a date for a sill associated with coals of the Williams Fork Formation (Cretaceous) in the Bowie area (near Paonia, CO) at 9.59±0.12 Ma, which is in the range of the GMVF dates.

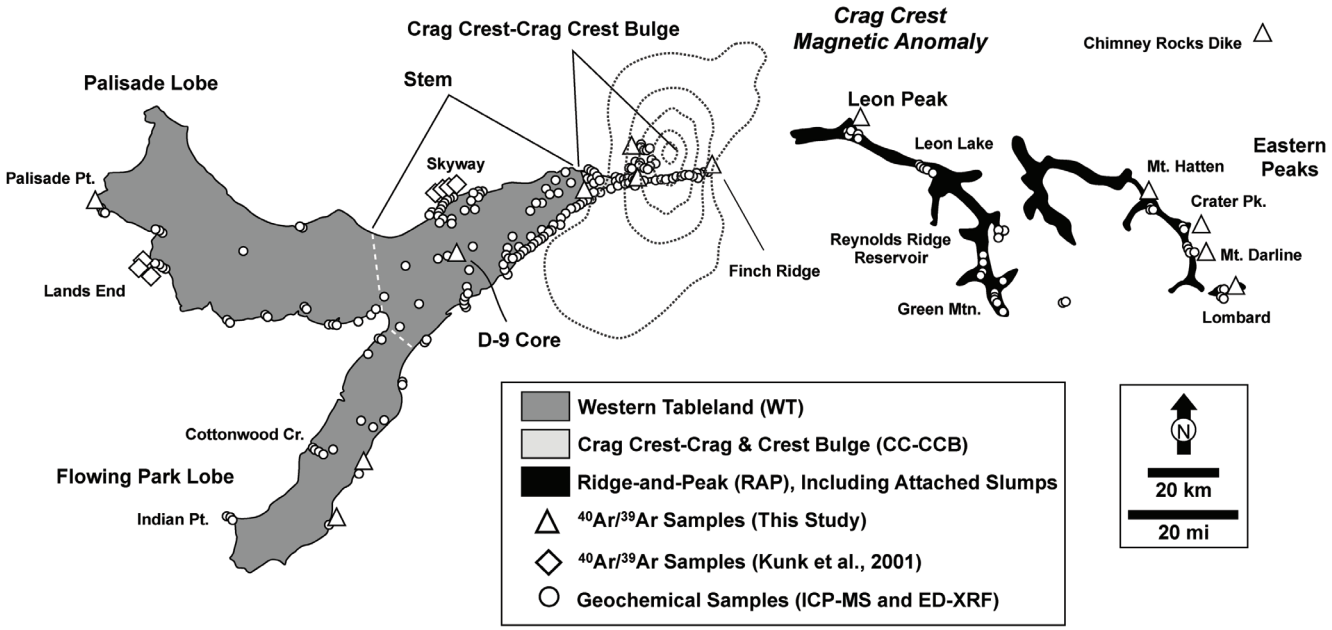

SAMPLES			
	DATE	ICP-MS	ED-XRF
WT	18	54	235
CC-CCB	4	14	95
RAP	9	13	74
Totals	31	81	404

FIGURE 3. Map of GMVF showing locations of samples used for $^{40}Ar/^{39}Ar$ dating and geochemical analyses by ICP-MS and ED-XRF. The dotted lines in the CC-CCB area outline a prominent positive aeromagnetic anomaly (Grauch and Plesha, 1989). The outlines for the flows in the RAP area include slump blocks that are attached to the intact flows. The insert table summarizes the samples collected from the three main areas of GMVF.

GEOCHEMISTRY

Methodology

The geochemistry part of this study includes 485 whole-rock samples collected from 46 locations (Fig. 3). Eighty-one samples were first analyzed for major-element oxides and trace elements by ICP-MS (inductively coupled plasma-mass spectroscopy) at ACTLabs (Ancaster, Ontario, Canada; 4 Lithoresearch package). The remaining 404 samples were analyzed at Colorado Mesa University (CMU) with a Bruker Tracer III-SD energy-dispersive fluorescence (ED-XRF) spectrometer (vacuum conditions) to determine major-oxide values.

For the ED-XRF analyses, cut slabs were positioned over the instrument's 4 by 5 mm port and irradiated (Rh source) at three or more random spots for one minute each. The instrument was configured to measure K-α1 peaks for Na, Mg, Al, Si, P, K, Ca, Ti, Mn, and Fe and calibrated with 25 cut slabs that had been analyzed by ICP-MS to convert the ED-XRF spectral peaks to major-element oxides in weight percent. The ED-XRF-oxide sums for each spot assay were typically between 95 and 105%. If the oxide sum exceeded these limits, data for that spot were discarded (1.6% were rejected). Following this qualification step, the oxide values from the spot assays for each sample were averaged to a single value. Since the calibration was developed from the ICP-MS data, the ED-XRF oxide values are considered acceptable for the geochemical mapping discussed below. It should be noted, however, that the ED-XRF sodium values were near the detection limit of the Bruker Tracer III-SD, so there is greater uncertainty for those data.

Results

Tabular and graphical comparisons of the major-element-oxide ICP-MS and ED-XRF data are given in Figure 6. The log-log plot of the mean oxide values for the two suites shows good agreement ($R^2 = 0.99$). Total-alkali (Na_2O+K_2O) vs. silica (SiO_2) plots also show similar groupings of data points, and illustrate that a variety of mafic to intermediate rocks are present. All samples are potassic. The majority of the samples are basalt or basaltic andesite, with less abundant potassic trachy basalt, shoshonite, and latite.

Geographic Variability

In Figure 7, the combined ED-XRF and ICP-MS data for each area are summarized in TAS plots, SiO_2 vs. K_2O plots, and histograms. These diagrams clearly show the unique composition of the CC-CCB samples compared to the WT and RAP groups, which are relatively similar to each other. The histograms show that the WT (N=289) are mostly medium-K and

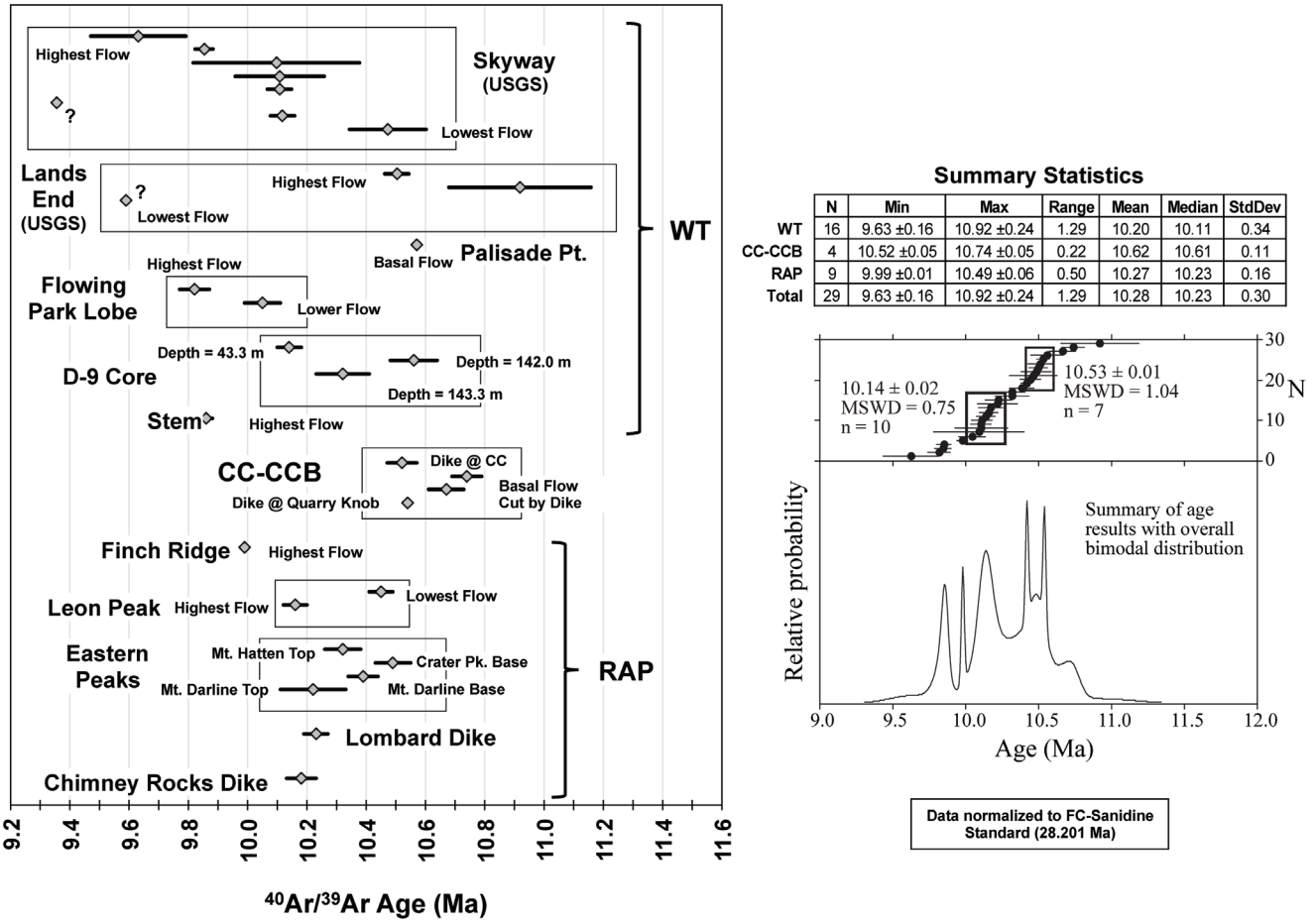

FIGURE 4. Summary of $^{40}Ar/^{39}Ar$ age dates for GMVF. Those from Skyway and Lands End are from Kunk et al. (2002); all of the other dates are from the present study (analyses at NMGRL). All dates are referenced to a Fish Canyon Tuff sanidine age of 28.201 Ma. The histogram uses a 0.2-Ma bin spacing. Note that the two youngest samples at Skyway and Lands End (with question marks) are not used in any of the statistical analyses. See text for discussion.

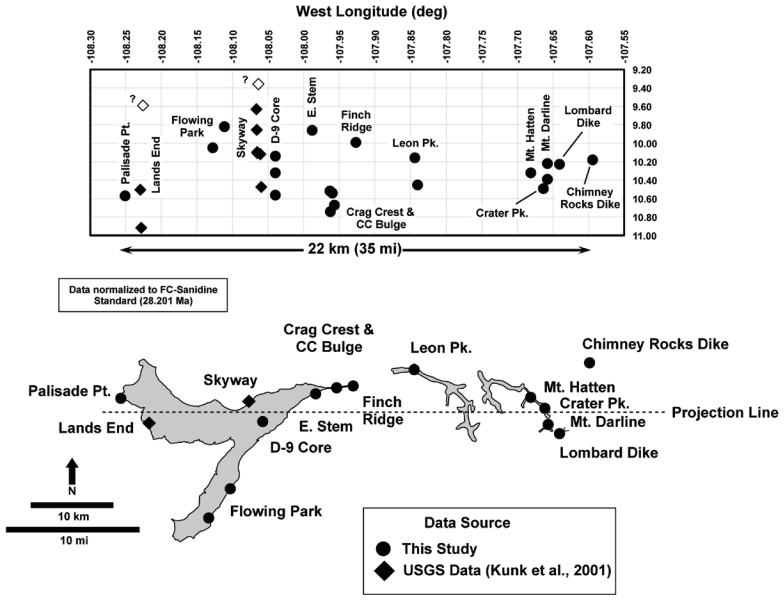

FIGURE 5. Plot of $^{40}Ar/^{39}Ar$ age dates for GMVF by geographic position. Samples have been projected on an east-west line according to longitude. All dates are referenced to a Fish Canyon Tuff sanidine age of 28.201 Ma. Note that the two youngest samples at Skyway and Lands End (with question marks) are not used in any of the statistical analyses. See text for discussion.

high-K basalt and basaltic andesite, with less abundant medium-K and high-K basalt, and only minor amounts of potassic trachy basalt and shoshonite. The RAP samples (N=87) are generally more potassic with a higher proportion of high-K basalt and basaltic andesite, potassic trachy basalt, and shoshonite. In striking contrast, the CC-CCB samples (N=109) are mainly shoshonite and latite. It should be noted that samples from the Lombard dike in the RAP area are geochemically similar to the samples at CC-CCB; however, the RAP flows are dissimilar.

Chemo-Stratigraphic Variability

The D-9 core, which is near the junction of PL and FPL (Fig. 3), provides the thickest known flow sequence (187.7 m) in the GMVF and was used to define chemo-stratigraphic variations for the WT area. As shown in Figure 8, the core contains least 26 flows ranging in thickness from 2.4 to 14.6 m. Individual flows commonly have dense bases and distinctly vesiculated tops that show both a'a and pahoehoe structures. Thin (0.3-2.5 m) interbeds (N=10) of red siltstone, silty claystone, and clayey

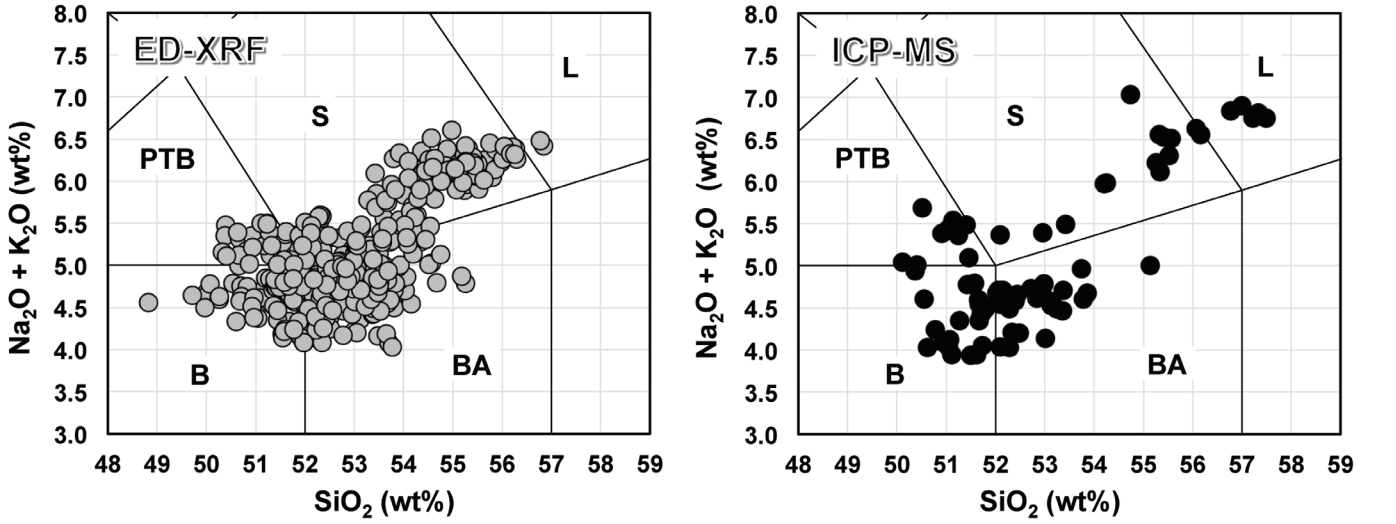

ED-XRF DATA (wt%)

	Na2O	MgO	Al2O3	SiO2	P2O5	K2O	CaO	TiO2	MnO	Fe2O3	Total
N	404	404	404	404	404	404	404	404	404	404	404
Min	3.03	2.41	14.84	48.82	-0.10	0.93	5.76	0.00	0.13	10.18	100
Max	3.27	9.87	15.63	56.84	1.08	3.47	10.45	1.85	0.17	11.83	100
Range	0.24	7.47	0.79	8.02	1.18	2.54	4.69	1.85	0.03	1.65	
Mean	3.13	5.82	15.32	52.99	0.50	2.03	7.62	1.58	0.15	10.87	100
Median	3.12	5.96	15.35	52.87	0.41	1.84	7.84	1.56	0.15	10.91	100
Std. Dev.	0.03	1.42	0.13	1.50	0.24	0.62	0.79	0.13	0.00	0.29	

ICP-S-MS DATA (wt%)

	Na2O	MgO	Al2O3	SiO2	P2O5	K2O	CaO	TiO2	MnO	Fe2O3	Total
N	81	81	81	81	81	81	81	81	81	81	81
Min	2.74	2.73	14.38	50.11	0.23	0.90	5.78	1.35	0.11	8.70	100
Max	3.62	8.48	16.18	57.49	1.17	3.42	9.26	1.87	0.17	12.53	100
Range	0.87	5.75	1.80	7.37	0.94	2.51	3.49	0.52	0.06	3.83	
Mean	3.10	6.24	15.32	52.77	0.49	1.94	7.53	1.57	0.15	10.90	100
Median	3.08	6.76	15.26	52.28	0.37	1.74	7.69	1.53	0.15	11.18	100
Std. Dev.	0.21	1.47	0.39	1.84	0.23	0.70	0.72	0.14	0.01	0.98	

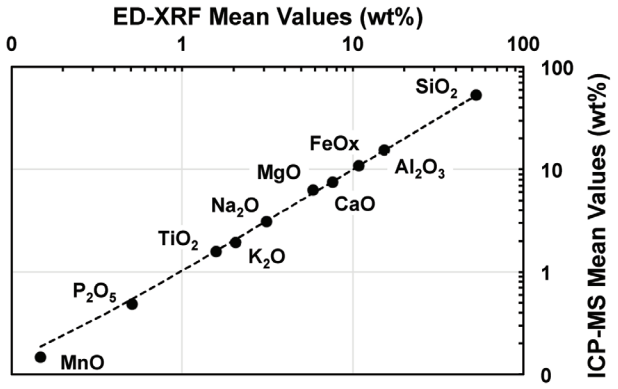

FIGURE 6. Comparison of geochemical data derived by ICP-MS (N=81) and ED-XRF (N=404). The insert table provides statistical summaries for the two data sets, and the plot in the lower right compares the mean values for various oxide values determined by the two methods. The R^2 value for the regression line is 0.99. The TAS (total-alkali-silica) plot shows similar data-point clouds, and that five compositional types are present: B, basalt; BA, basaltic andesite; PTB, potassic trachy basalt; S, shoshonite; and L, latite.

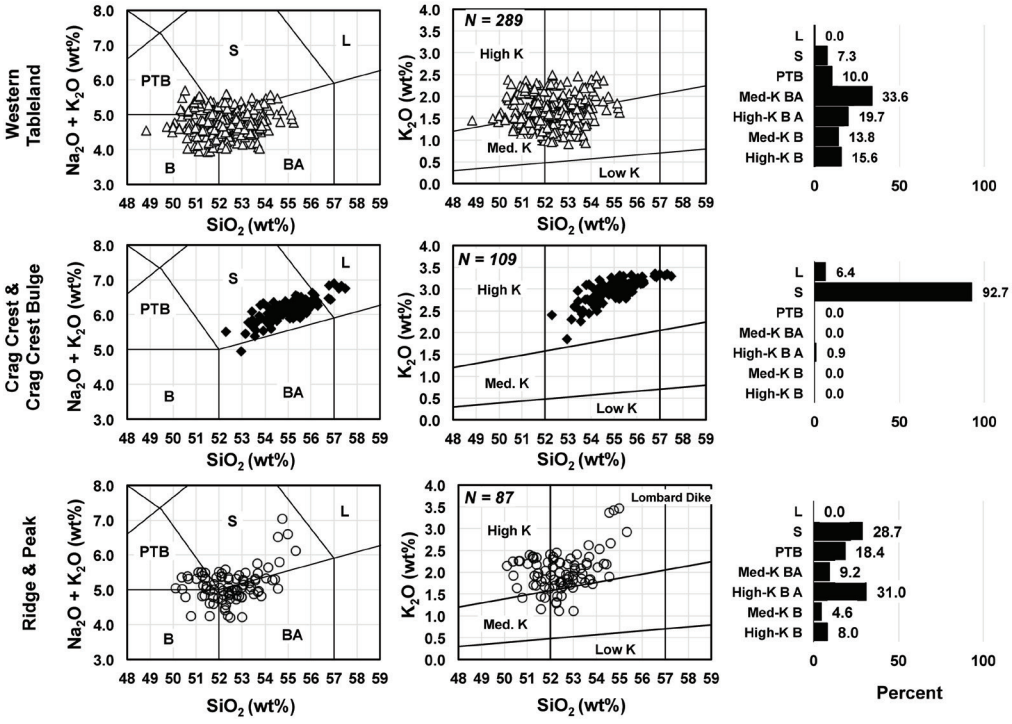

FIGURE 7. Summary of compositional data for all ICP-MS and ED-XRF samples from the WT, CC-CCB, and RAP areas. TAS plots are on the left; abbreviations are explained in Figure 6. The K_2O vs. SiO_2 plots (middle) define low-, medium-, and high-potassium terms for basalts and basaltic andesites. Histograms on right show the percentages of various rock types when the TAS and potassium-enrichment terms are combined.

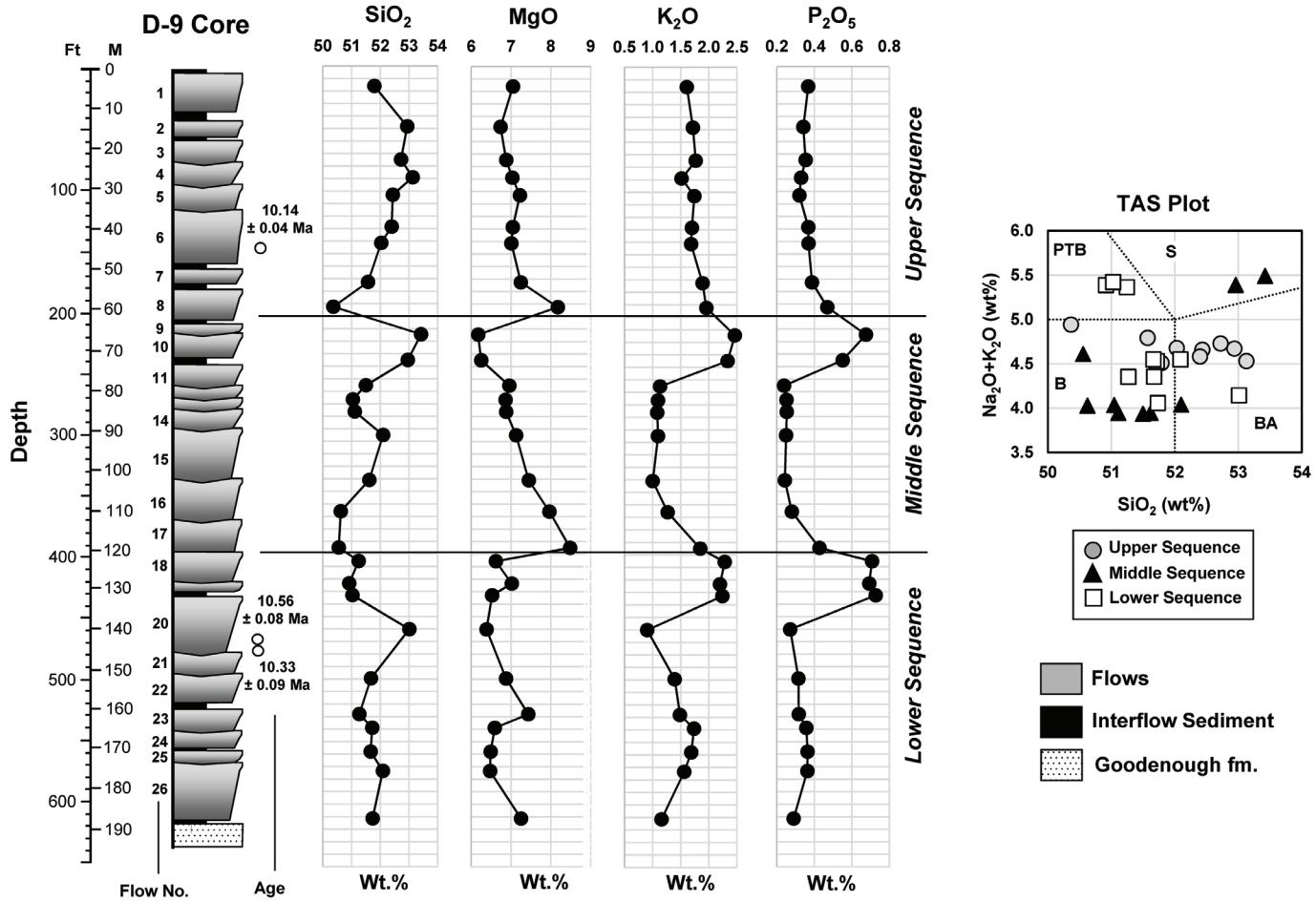

FIGURE 8. Chemo-stratigraphic variations for selected oxide values for the D-9 core (39º 1.69'N; 108º 3.80'W; 3095 m elevation). The core, which includes 26 flows and 10 claystone-siltstone-limestone interbeds, is the thickest documented sequence in the GMVF. The chemo-stratigraphic plots for P_2O_5, MgO, K_2O, and SiO_2 (ICP-MS analysis) define three sequences. The TAS plot shows that most samples are basalt or basaltic andesite; however, flows 18 and 19 are more alkali-rich potassic trachy basalt and flows 9 and 10 are shoshonite. See text for discussion. Abbreviations are explained in Figure 6.

limestone also occur, suggesting that significant periods of time (possibly up to 100 kyr or more) may have occurred between subsequent flow emplacements. Three $^{40}Ar/^{39}Ar$ ages from the core range from 10.56±0.08 to 10.14±0.04 Ma.

For geochemical analysis, the densest part of each flow in the D-9 core was sampled. The stratigraphic variations of the SiO_2, K_2O, MgO, and P_2O_5 values from the ICP-MS analyses show the presence of three geochemical sequences (Fig. 8). The sequence boundaries are defined by abrupt increases in MgO concentration, and the lower and middle sequences are capped by more alkaline potassic trachy basalt or shoshonite. The lower sequence (9 flows with a composite thickness of 65.1 m) may have two subsequences that show upward decreases in MgO concentration with relatively uniform K_2O and P_2O_5 concentrations. The uppermost samples (flow 18 and 19) in the lower sequence are potassic trachy basalt with significantly higher K_2O and P_2O_5 values compared to the medium-K basalt and basaltic andesite found lower in the sequence. The middle sequence (9 flows with a composite flow thickness of 53.3 m) shows a similar pattern. The basal sample (flow 17) is a Mg-rich basalt (8.5 wt% MgO), whereas the upper two samples (flows 9 and 10) are K_2O- and P_2O_5-rich shoshonites. These two samples, however, are not as evolved as the shoshonites from the CC-CCB area (Fig. 7). Other samples in the middle sequence are medium-K basalt and basaltic andesite; however, decreasing K_2O and P_2O_5 concentrations in the lower part of the sequence may indicate mixing with older, more alkaline magmas. The upper sequence (8 flows with a composite thickness of 55.6 m) shows a similar pattern with a Mg-rich basalt (8.2 wt% MgO) defining its base (flow 8) and decreasing K_2O and P_2O_5 in the lower part of the sequence. Most of the samples in the upper sequence are high-K basalt and basaltic andesite.

The chemo-stratigraphic variations shown in Figure 8 suggest that both magmatic differentiation and the introduction of more mafic magmas with variable composition occurred during emplacement of some WT flows.

VENT AREAS

Young and Young (1968) suggested that the GMVF magma may have come from the LP area and/or from fissure eruptions, now represented by the large east-west-trending dikes at CRR, LR, and LDC (Fig. 2). These suggestions were never con-

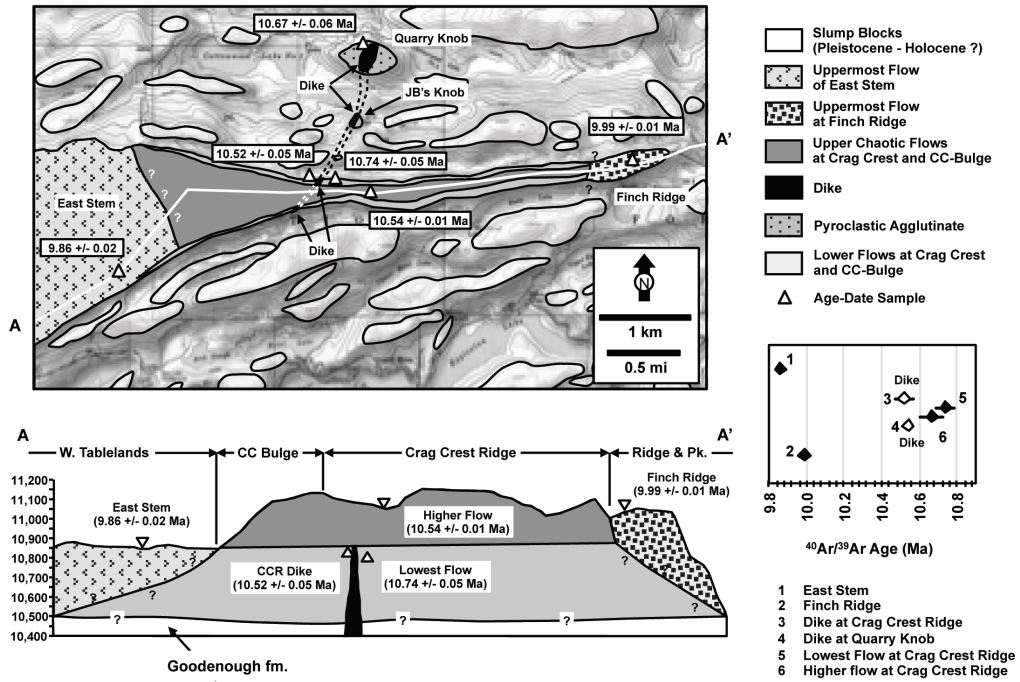

FIGURE 9. Sketch map and diagrammatic cross section of the CC-CCB area and the easternmost part of the WT area ("East Stem") and the westernmost part of the RAP area (Finch Ridge). A major dike and associated agglutinated pyroclastics occurs between Quarry Knob and Crag Crest Ridge. The dike does not completely penetrate the upper flow sequence. The dates for the dike and associated flows cluster near 10.5 Ma; however, dates for the uppermost flows at East Stem and Finch Ridge are younger by about 0.6 Ma. There is a significant compositional difference between the CC-CCB samples and those immediately to the east and west (Fig. 7). See text for discussion.

firmed. In 2002, based on an observation by John Trammell, a vent complex was discovered on a small, reddish hill (147 m high) between Cottonwood No. 1 and Cottonwood No. 4 Reservoirs and Lily Lake (Fig. 9). Mapping of this hill, herein called "Quarry Knob" (QK), showed that it consists of red to pink pyroclastics (agglutinated ash, cinders, and small bombs) associated with three southwest-trending, near-vertical dikes up to 40 m across. One of the QK dikes continues southwest to "JB's Knob" (JBK) where it is about 25 m wide and near vertical. The east side of the JBK dike has minor red agglutinate and a well-defined chill zone with columnar jointing on the west flank. The next occurrence of the dike is at CCR, where it is about 15 m wide, near vertical, and has columnar jointing on both sides. The CCR dike intrudes into a 45 m thick series of lower flows (base not exposed), but does not cut through the upper part of the sequence, which consists of 60-90 m of small, highly contorted, pahoehoe-type flows, and gray agglutinate (rare). This upper (un-intruded) sequence forms CCB and the upper half of CCR. The CC-CCB complex is located on the western flank of a prominent positive aeromagnetic anomaly (Fig. 3) shown on a regional map by Grauch and Plesha (1989).

Four $^{40}Ar/^{39}Ar$ dates were established for the CC-CCB complex (Table 1, Fig. 9). The QK dike is 10.67± 0.06 Ma and the CCR dike is 10.52±0.05 Ma. A sample from a flow cut by the CCR dike is 10.74±0.05 Ma, and a sample from a contorted flow near the top of CCR is 10.54±0.01 Ma. Dates from the eastern stem and Finch Ridge, which are about the same elevation, are noticeably younger (9.86±0.02 and 9.99±0.01 Ma, respectively). The ICP-MS and ED-XRF data for the CC-CCB area are also noticeably different from the WT and RAP areas (Fig. 7). Almost all the CC-CCB samples are shoshonite or latite, with minor basaltic andesite. Although talus partly obscures the lower flanks of the area, the geochemical boundary between the CC-CCB area, the eastern stem of the WT area, and the westernmost part of the RAP area (i.e., Finch Ridge) appears to be sharply defined. Thus, it is suggested that the CC-CCB eruptions formed a dome or small shield volcano that younger lavas in the WT and RAP areas flowed around.

Geochemical correlation of the flows and dikes in the WT and RAP area with the CC-CCB vent complex are uncertain. In the D-9 core, flows 9 and 10 are shoshonite (Fig. 8); however, the enrichment in SiO_2, K_2O, and P_2O_5 is not as high as in the CC-CCB samples. A correlation between CC-CCB and LP is also possible. LP lies about 10.6 km east of the CC-CCB complex (Figs. 2 and 3) and consists of nine flows with a total thickness of about 137 m. The lowest exposed flow at LP is dated at 10.45±0.04 Ma and the highest flow is 10.16±0.04 (Table 1). Flow 6, which is near the middle of the LP sequence, is a shoshonite; however, LP samples above and below are dissimilar. The connection between the CC-CCB complex and the flows in the eastern RAP area (MD, MH, CP) and the LR dike (Fig. 4) is also uncertain. All of the dates from flows in the eastern RAP area are between 10.49±0.06 and 10.23±0.11 Ma (Fig. 5) and are similar to those at CC-CCB; however, all of the flows in this area are not enriched in any of the oxides that characterize the CC-CCB samples. The LR dike, which is dated at 10.23±0.04 Ma and cross-cuts flows near MD, is enriched in SiO_2, Na_2O, and K_2O (Fig. 7) but is slightly younger than any dates at CC-CCB.

SUMMARY

The upper parts of Grand Mesa document the remains of one of the largest late Cenozoic basaltic lava fields in western Colorado, and is subdivided into three areas (WT, CC-CCB, and RAP). $^{40}Ar/^{39}Ar$ dates (N=29) for the total field range from 10.92±0.24 to 9.63±0.16 Ma (mean=10.28 Ma), and show an overall bimodal distribution. Dikes and flows in the RAP area cluster between 10.49±0.06 to 9.99±0.01 Ma, where-

as the dikes and flows in the CC-CCB area cluster between 10.74±0.05 to 10.52±0.05 Ma. Flows of the WT area are more variable, ranging from 10.92±0.24 to 9.63±0.16 Ma. Major-element-oxide values from both ICP-MS analyses (N=81) and ED-XRF analyses (N=404) show geographic partitioning. Samples from the CC-CCB area are dominated by shoshonite and latite, compared to the medium- to high-K basalt and basaltic andesite samples that dominate the WT and RAP samples. The distribution of the CC-CCB samples coincides with a large positive aeromagnetic anomaly. Major-element-oxide values also show chemo-stratigraphic variations, as expressed in flows from the D-9 core. These variations suggest that both magmatic differentiation and the introduction of more mafic magmas with variable composition occurred during the eruptive history. The CC-CCB area has the only well-defined vent complex, consisting of a major dike and scattered pyroclastics. Ages for the dike and associated flows are tightly constrained between 10.74±0.05 and 10.52±0.05 Ma, and the geochemical composition is uniform. The chronological and geochemical correlation of this complex to flows in the WT and RAP is not well understood. Additional unknown vent areas are likely present.

ACKNOWLEDGMENTS

This effort has been significantly enhanced by many individuals. Robert Young (deceased) and John Trammell provided insight that helped guide the early field work. Karl Karlstrom provided support and encouragement for many aspects of the project. Thanks also to Ken Weston and Joe Barnes who provided geotechnical information on cores taken by the U.S. Bureau of Reclamation, and Andres Aslan who provided the date at Palisade Point. Verner Johnson was very helpful in the GIS/GPS aspects of the project. Former and current CMU students involved include Andy Darling, Ian Shafer, Ronni Whittle, Rachael Lohse, Mickey Guziak, and Walter Green. Western State Colorado University (WSCU) students include Tanya Chuprikova, Judy Esposito, Caitlyn Harrington, Kevin McCall, Clare Pitcher, and Tom Sunderland. Logistical assistance to Cole was provided by Jim Brown, Art Trevena, and Joyce Tanihara. Funding sources included the CREST Project (NSF), via Karl Karlstrom, Faculty Professional Development Grants by CMU and WSCU to Cole and Stork, the Unconventional Energy Center at CMU, the Grand Junction Geological Society, as well as peripheral donations from several petroleum companies and private foundations to support CMU's mineralogy and geochemistry lab. Art Trevena and Cassandra Fenton provided constructive pre-submittal technical reviews. Thank you.

REFERENCES CITED

Aslan, A., Karlstrom, K., Hood, W., Cole, R., Oesleby, T., Betton, C., Sandoval, M., Darling, A., Kelley, S., Hudson, A., Kaproth, B., Schoepfer, S., Benage, M., and Landman, R., 2008, River incision histories of the Black Canyon of the Gunnison and Unaweep Canyon: Interplay between late Cenozoic tectonism, climate change, and drainage integration of the western Rocky Mountains, *in* Raynolds, R.G., ed., Roaming the Rocky Mountains and Environs: Geological Field Trips: Boulder, Colorado, Geological Society of America Field Guide 10, p. 175-202, doi: 10.1130/2008.fld010(09).

Aslan, A., Karlstrom, K.E., Crossey, L.J., Kelley, S., Cole, R., Lazear, G., and Darling, A., 2010, Late Cenozoic evolution of the Colorado Rockies: Evidence for Neogene uplift and drainage integration, *in* Morgan, L.A., and Quane, S.L., eds., Through the Generations: Geologic and Anthropogenic Field Excursions in the Rocky Mountains from Modern to Ancient: Boulder, Colorado, Geological Society of America Field Guide 18, p. 21-54, doi: 10.1130/2010.0018(02).

Baum, R.L., and Odum, J.K., 1996, Geologic map of slump-block deposits in part of the Grand Mesa area, Delta and Mesa Counties, Colorado: U.S. Geological Survey Open-file Report 96-017, 12p., 2 plates, scale 1:24,000.

Baum, R.L., and Odum, J.K., 2003, Retrogressive slumping at Grand Mesa Colorado, *in* Boyer, D.D., Santi, P.S., and Rogers, W.P., eds., Engineering Geology in Colorado: Contributions, Trends and Case Histories: Association of Engineering Geologists Special Publication No. 15 and Colorado Geological Survey Special Publication 55, (CD-ROM), 17 p.

Baum, R.L., Lidke, D.J., and Hart, M. 2007, Grand Mesa landslide complex, *in* Noe, D.C., and Coe, J.A., eds., Field Trip Guidebooks, 1st North American Landslide Conference: Association of Environmental and Engineering Geologists Special Publication 21 and Colorado Geological Survey Special Publication 56, 25 p.

Budahn, J.R., Unruh, D.M., Kunk, M.J., Byers, F.M., Jr., Kirkham, R.M., and Streufert, R.K., 2002, Correlation of late Cenozoic basaltic lava flows in the Carbondale and Eagle collapse centers in west-central Colorado based on geochemical, isotopic, age, and petrographic data, *in* Kirkham, R.M., Scott, R.B., and Judkins, T.W., eds., Late Cenozoic Evaporite Tectonism and Volcanism in West-Central Colorado: Boulder, Colorado, Geological Society of America Special Paper 366, p. 167-196.

Cole, R.D., 2011, Significance of the Grand Mesa basalt field in western Colorado for defining the early history of the upper Colorado River, *in* Beard, L.S., Karlstrom, K.E., Young, R.A., and Billingsley, G.H., eds., CRevolution 2 -- Origin and Evolution of the Colorado River System, Workshop Abstracts: U.S. Geological Survey Open-file Report 2011-1210, p. 55-61.

Cole, R.D., Heizler, M., Karlstrom, K.E., and Stork, A., 2010, Eruptive history of the Grand Mesa basalt field, western Colorado (abs.): Geological Society of America Abstracts with Programs, v. 42, no. 5, p. 76.

Cole, R.D., Hood, W.C., Aslan, A., and Borman, A., 2013, Stratigraphic, sedimentologic, and mineralogical characterization of the Goodenough Formation (Miocene?), Grand Mesa, CO (abs.): Geological Society of America Abstracts with Programs, v. 45, no. 7, p. 242.

Cole, R.D., Stork, A., and Hood, W.C., 2016, Geochemical variation of Grand Mesa Volcanic Field, western Colorado (abs.): Geological Society of America Abstracts with Programs, v. 48, no. 7, Paper 315-5, doi: 10.1130/abs/2016AM-283767.

Day, W.C., and Bove, D.J., 2004, Review of the geology of western Colorado, *in* Bankey, V., ed., Resource Potential and Geology of the Grand Mesa, Uncompahgre, and Gunnison (GMUG) National Forests and Vicinity, Colorado: U.S. Geological Survey Bulletin 2213-B, p. 11-36.

Grauch, V.J.S., and Plesha, J.L., 1989, Aeromagnetic maps of the Uinta and Piceance Basins and vicinity, Utah and Colorado: U.S. Geological Survey, Miscellaneous Field Studies Map MF-2008-C, scale 1:500,000.

Green, W.S., and Cole, R.D., 2016, Reconstruction of Grand Mesa Volcanic Field, western Colorado (abs.): Geological Society of American Abstracts with Programs, v. 48, no. 7, Paper 59-11, doi: 10.1130/abs/2016AM-284000.

Karlstrom, K.E., Whitmeyer, S.J., Dueker, K., Williams, M.L., Bowring, S.A., Levander, A.R., Humphreys, E.D., Keller, G.R., and the CD-ROM Working Group, 2005, Synthesis of results of the CD-ROM experiment: 4-D image of the lithosphere beneath the Rocky Mountains and implications for understanding the evolution of continental lithosphere, *in* Karlstrom, K.E. and Keller, G.R., eds., The Rocky Mountain Region: an Evolving Lithosphere, Tectonics, Geochemistry, and Geophysics: American Geophysical Union Geophysical Monograph Series 154, p. 421-441, doi: 10.1029/154GM31.

Karlstrom, K.E., Coblentz, D., Dueker, K., Ouimet, W., Kirby, E., Van Wijk, J., Schmandt, B., Kelley, S., Lazear, G., Crossey, L.J., Crow, R., Aslan, A., Darling, A., Aster, R., MacCarthy, J., Hansen, S.M., Stachnik, J., Stockli, D.F., Garcia, R.V., Hoffman, M., McKeon, R., Feldman, J., Heizler, M., Donahue, M.S., and the CREST Working Group, 2012, Mantle-driven

dynamic uplift of the Rocky Mountains and Colorado Plateau and its surface response: Toward a unified hypothesis: Lithosphere, v. 4, p. 3-22, doi:10.1130/L150.1.

Kunk, M. J., and Snee, L.W., 1998, $^{40}Ar/^{39}Ar$ age-spectrum data of Neogene and younger basalts in west central Colorado: U. S. Geological Survey Open-file Report 98-243, 112 p.

Kunk, M.J., Winick, J.A., and Stanley, J.O., 2001, $^{40}Ar/^{39}Ar$ age-spectrum and laser fusion data for volcanic rocks in west central Colorado: U.S. Geological Survey Open-file Report 01-472, 94 p.

Kunk, M.J., Budahn, J.R., Unruh, D.M., Stanley, J.O., Kirkham, R.M., Bryant, B., Scott, R.B., Lidke, D.J., and Streufert, R.K., 2002, $^{40}Ar/^{39}Ar$ ages of late Cenozoic volcanic rocks within and around the Carbondale and Eagle collapse centers, Colorado: Constraints on the timing of evaporite-related collapse and incision of the Colorado River, *in* Kirkham, R.M., Scott, R.B., and Judkins, T.W., eds., Late Cenozoic Evaporite Tectonism and Volcanism in West-Central Colorado: Boulder, Colorado, Geological Society of America Special Paper 366, p. 213-234.

Larson, E.E., Ozima, M., and Bradley, W.C., 1975, Late Cenozoic basic volcanism in northwestern Colorado and its implications concerning tectonism and the origin of the Colorado River system, *in* Curtis, B.F., ed., Cenozoic History of the Southern Rocky Mountains: Boulder, Colorado, Geological Society of America Memoir 144, p. 155-178.

Leat, P.T., Thompson, R.N., Morrison, M.A., Hendry, G.L., and Dickin, A.P., 1988, Compositionally diverse Miocene-Recent rift-related magmatism in northwest Colorado: Partial melting and mixing of mafic magmas from 3 different asthenospheric and lithospheric mantle sources: Journal of Petrology, Special Volume 1, Physical and Chemical Properties of the Lithospehere, p. 351-377.

Leat, P.T., Thompson, R.N., Dickin, A.P., Morrison, M.A., and Hendry, G.L., 1989, Quaternary volcanism in northwestern Colorado: Implications for the roles of asthenosphere and lithosphere in the genesis of continental basalts: Journal of Volcanology and Geochemical Research, v. 37, p. 291-310.

Marvin, R.F., Mehnert, H.H., and Mountjoy, W.M., 1966, Age of basalt cap on Grand Mesa, *in* Geological Survey Research 1966: U.S. Geological Survey Professional Paper 550-A, p. A81.

Robeck, E.D., 2005, The effects of fault-induced stress anisotropy on fracturing, folding, and sill emplacement: Insights from the Bowie coal mines, southern Piceance Basin, western Colorado (M.S. thesis): Provo, Brigham Young University, 94 p.

Stork, A.L., 2006, Petrology and geochemistry of the Red Mountain and Flat Top basalts, Gunnison County, Colorado (abs.): Geological Society of America Abstracts with Programs, v. 38, no. 6, p. 4.

Tweto, O., Moench, R.H., and Reed, J.C., Jr., 1976a, Preliminary geologic map of the Leadville 1º x 2º quadrangle, northwestern Colorado: U.S. Geological Survey Miscellaneous Field Studies Map MF-760, scale 1:250,000.

Tweto, O., Steven, T.A., Hail, W.J., Jr., and Moench, R.H., 1976b, Preliminary geologic map of the Montrose 1º x 2º quadrangle, southwestern Colorado: U.S. Geological Survey Map MF-761, scale 1:250000.

Tweto, O., 1979, Geologic map of Colorado: U.S. Geological Survey Special Geologic Map, scale 1:500,000.

Unruh, D.M., Budahn, J.R., Siems, D.F., and Byers, F.M., Jr., 2001, Major- and trace-element geochemistry; lead, strontium, and neodymium isotopic compositions; and petrography of late Cenozoic basaltic rocks from west-central Colorado: U.S. Geological Survey Open-file Report 01-477, 83 p.

Yeend, W.E., 1969, Quaternary geology of the Grand and Battlement Mesas area, Colorado: U.S. Geological Survey Professional Paper 617, 50 p.

Yeend, W.E., 1973, Slow-sliding slumps, Grand Mesa, Colorado: The Mountain Geologist, v. 10, no. 1., p. 25-28.

Young, R.G., and Young, J.W., 1968, Geology and Wildflowers of Grand Mesa, Colorado: Grand Junction, Wheelwright Press, 160 p.

Supplemental data can be found at http://nmgs.nmt.edu/repository/index.cfml?rid=2017004